Evaluation of entrainment of a nonlinear neural oscillator to white noise

Jason Ritt*
McGovern Institute for Brain Research, MIT E25-414, Cambridge, Massachusetts 02139, USA
(Received 23 July 2003; published 29 October 2003)

The Lyapunov exponent for a one-dimensional neural oscillator model, the theta neuron, is computed for white noise forcing, using the steady-state solution to the associated Fokker-Planck equation. The latter is mildly singular, due to the nature of the multiplicative input. In agreement with previous results with similar models, the exponent is negative for all forcing amplitudes, but here it is shown to be small, relative to that for periodic drive, in a range of forcing strengths. Thus the synchronization of an ensemble of independent neurons receiving common but random input can be slow. Moreover, this implies that aperiodic input may be suboptimal, in some contexts, for preserving the reliability of fine spike timing, a potentially important component of the neural ''code.''

DOI: 10.1103/PhysRevE.68.041915 PACS number(s): 87.10.+e, 05.40.−a, 87.17.Nn

I. INTRODUCTION

Cortical neurons *in vivo* receive thousands of synaptic inputs, the sum of which resembles a white or low-pass filtered ''noise'' input [1–3]. It is now well established that neurons can entrain to such inputs, in the sense that, if an identical realization of the input is repeatedly applied, the resultant neural output (spike trains or membrane potential time series) is nearly identical from trial to trial [3–9]. The degree of similarity between trials, specifically in the timing of action potentials, is called the spike time *reliability*. Due to intrinsic (e.g., channel) noise, reliability is typically poor in the absence of input fluctuations [3,7,10].

In most theoretical investigations of reliability, each trial is modeled as the response of a different neuron in an uncoupled ensemble of identical neurons receiving a global input [11–15]. The ensemble evolves in a common (nonautonomous) phase space, and reliable firing is equivalent to synchronization of the ensemble. It has been argued that reliable spike responses to broadband ''aperiodic'' inputs are generic, in both excitable and oscillatory neuron models, and do not depend on the fine details of the driving signal or the neural kinetics [12,15,16]. Indeed, under fairly mild assumptions, all one-dimensional stochastic differential equations are stable in the sense of having a negative Lyapunov exponent ([17], Sec. 9.2.2), which suggests that the solutions typically converge asymptotically to a small number of distinct solutions [12]. A similar result has been found numerically in two dimensions, although a small subset of parameters led to chaotic behavior [15].

However, for neural oscillators it is well known that periodic inputs must be tuned to appropriate frequencies for entrainment (hence reliability) to occur. Further, [7,9] show, both in experiments on *Aplysia* motoneurons and simulations of an integrate and fire model, that reliability under a broadband input can be substantially reduced when that input is notch filtered around the oscillator frequency, a behavior they termed *reliability resonance*. Importantly, the effect of reliability resonance is amplitude dependent. Similar results have been observed in cortical slices [8]. Thus, reports of the generality of aperiodic response reliability, while not incorrect, may overstate the importance of this result to biophysical function, and miss frequency dependent mechanisms that could affect reliable responses in functional networks [9,11,13]. A better understanding of the interaction between the input spectrum and the neural kinetics depends in part on quantitative comparisons of the efficacy of different inputs, including broadband and rhythmic signals, in driving reliable responses.

This paper determines the rate of ensemble synchronization, via the Lyapunov exponent (LE), for a one-dimensional neural oscillator model with broadband input. The exponent is always nonpositive, in agreement with previous studies, but can be small compared to that for periodic forcing. Thus in some regimes input coherence may be important to induce reliable spike timing.

II. THE THETA NEURON

The theta neuron equation,

$$\frac{d\theta}{dt} = 1 - \cos(\theta) + [1 + \cos(\theta)]I_{\text{app}} \tag{1}$$

is a normal form for a saddle node on a circle bifurcation, to which a large class of conductance based neural models (so called type I) can be reduced [18–20]. θ represents the phase of the voltage and conductance trajectory during a single spike cycle, and I_{app}, which is assumed small but not necessarily constant, is the total input (e.g., synaptic) current. By construction, the neuron ''spikes'' whenever $\theta = \pi$. When $I_{\text{app}} > 0$ the neuron is oscillatory, with period $\pi/\sqrt{I_{\text{app}}}$ (when I_{app} is constant). Otherwise the neuron is excitable, with a stable/unstable pair of fixed points around the origin [19].

For our purposes, two important physiological properties captured in the model are (i) nonuniform motion, consisting of slow motion around $\theta = 0$ and fast spiking as θ passes through π, and (ii) a decreasing influence of the input as the neuron reaches the spike (at $\theta = \pm\pi$, the term including I_{app} equals zero). This latter behavior corresponds to the physical

*Electronic address: jritt@mit.edu

notion that, during a spike, the high conductance of the spiking currents completely overwhelms the input [18,19].

This paper focuses on the oscillatory regime. The oscillatory theta neuron is similar to the active rotator model [12,21]; a key difference is the multiplicative input, which captures the substantially reduced input efficacy during the high conductance state of the spike. We imagine a cell receiving a mixture of excitatory and inhibitory synaptic currents, with a net depolarizing effect leading to oscillation, i.e., I_{app} has a positive mean (in typical experiments [3,7,9], a fluctuating current riding a positive dc bias is injected by an electrode). In the idealized limit of a large number of independent but smooth synaptic currents [2,3], I_{app} becomes ''white forcing,'' interpreted in the sense of Stratonovich [22]. The input is thus $I_{\text{app}}=u+\sigma\circ dW$ where $u>0$ is the mean, $\circ dW$ is the (Stratonovich) white noise differential, and σ is the forcing amplitude. Equation 1 becomes the stochastic differential equation (SDE)

$$d\theta = f(\theta)dt + g(\theta)\circ dW, \tag{2}$$

where

$$f(\theta) = 1-\cos(\theta)+[1+\cos(\theta)]u, \tag{3a}$$

$$g(\theta) = [1+\cos(\theta)]\sigma. \tag{3b}$$

We define the *natural period* as $T_N \equiv \pi/\sqrt{u}$, i.e., the period when $\sigma=0$.

We will utilize the probability density $\rho(\theta,t)$ of oscillator phases, which is governed by the Fokker-Planck equation. In the steady state, ρ gives the distribution both over all initial phases and over all realizations of the input. Information about the distribution of solutions with different initial conditions but forced by the same realization of the input is then derived from the Lyapunov exponent (see below) [17]. To find the Fokker-Planck equation associated with Eq. (2), it is first necessary to write the SDE in Itô form [22],

$$d\theta = \left(f(\theta)+\frac{1}{2}g(\theta)g'(\theta)\right)dt + g(\theta)dW, \tag{4}$$

where the prime indicates differentiation with respect to θ, and the stochastic differential dW is of Itô type. The corresponding Fokker-Plank equation is then [22]

$$\frac{\partial\rho}{\partial t} = -\frac{\partial}{\partial\theta}\left\{\left(f+\frac{1}{2}gg'\right)\rho\right\}+\frac{1}{2}\frac{\partial^2}{\partial\theta^2}\{g^2\rho\}. \tag{5}$$

Under general conditions (including $\sigma>0$) every solution of this second order parabolic equation tends to a unique steady state, given by setting $\partial\rho/\partial t=0$. Note, however, that the equation is mildly singular $[g(\pm\pi)=0]$ due to the spike nonlinearity.

III. LYAPUNOV EXPONENT

A. The Fokker-Plank steady state

We first derive an integral expression for the steady-state solution ρ to the Fokker-Plank equation. While the general approach is standard [17,22], the singular point of Eq. (5) at the spike introduces some modifications. In the next section we compute the LE using ρ.

To find the steady state, consider

$$0 = -\frac{d}{d\theta}\left\{\left(f+\frac{1}{2}gg'\right)\rho\right\}+\frac{1}{2}\frac{d^2}{d\theta^2}\{g^2\rho\} \tag{6}$$

on the open interval $I\equiv(-\pi,\pi)$ on which the equation is nonsingular, along with the conditions (i) $\lim_{\theta\to-\pi}\rho(\theta) = \lim_{\theta\to\pi}\rho(\theta)$ and (ii) $\int_I\rho=1$. The first (boundary) condition restricts us to periodic solutions, and the second normalizes the solution to a probability density.

Integrating once yields

$$\frac{g^2}{2}\frac{d\rho}{d\theta}+\left(\frac{1}{2}gg'-f\right)\rho = C \tag{7}$$

with C to be determined. We define F (on I) via

$$F(\theta)\equiv\int_0^\theta\frac{2f(\eta)}{g^2(\eta)}d\eta = \frac{2}{\sigma^2}\tan\left(\frac{\theta}{2}\right)\left[\frac{1}{3}\tan^2\left(\frac{\theta}{2}\right)+u\right]$$

and the integrating factor as

$$\mu(\theta)\equiv\frac{1}{g(\theta)}\exp[-F(\theta)]. \tag{8}$$

Direct calculation shows that Eq. (7) is equivalent to

$$\frac{d}{d\theta}\left\{\mu\frac{g^2}{2}\rho\right\} = C\mu;$$

hence

$$\mu(\theta)\frac{g^2(\theta)}{2}\rho(\theta) = \sigma\rho_0 + C\int_0^\theta\mu(\eta)d\eta. \tag{9}$$

Above we used $\mu(0)=1/(2\sigma)$, $g(0)=2\sigma$, and the definition $\rho(0)\equiv\rho_0$. C and ρ_0 are not independent for the solution to satisfy the boundary condition. Suppose for the remainder that ρ_0 is fixed (at an as yet unknown value such that the solution has unit area); it remains to determine the corresponding C.

Under the change of variables $z=\tan(\theta/2)$ on $-\pi<\theta<\pi$, Eq. (8) becomes

$$\tilde{\mu}(z) = \frac{z^2+1}{2\sigma}\exp\left[-\frac{2}{\sigma^2}z\left(\frac{1}{3}z^2+u\right)\right] \tag{10}$$

on $-\infty<z<\infty$. Clearly, $\lim_{\theta\to-\pi}\mu=\lim_{z\to-\infty}\tilde{\mu}=\infty$ and $\lim_{\theta\to\pi}\mu=\lim_{z\to\infty}\tilde{\mu}=0$. This latter limit further implies that the integral of μ converges at the right end of the interval, so we define

$$\int_0^\pi\mu(\eta)d\eta\equiv M>0. \tag{11}$$

Now consider the limit $\theta \to \pi$ in the solution Eq. (9). Assuming that ρ is bounded, the left hand side goes to zero, which is a direct consequence of the spike singularity. Therefore for the equation to hold on all of I it is necessary that

$$C = -\frac{\sigma \rho_0}{M}, \tag{12}$$

and the only bounded steady-state solution on I is

$$\rho(\theta) = \frac{2\sigma\rho_0}{M} \frac{\int_\theta^\pi \mu(\eta) d\eta}{g^2(\theta)\mu(\theta)}, \quad -\pi < \theta < \pi. \tag{13}$$

In this expression, the integral limits have changed after simplification using the definition of M.

Since the derivation so far has invoked only the boundedness of ρ, it should be checked that this solution in fact approaches finite values at the two end points, and that these values are equal. For convenience, we rescale the solution as $r(\theta) = M\rho(\theta)/(2\sigma\rho_0)$ before taking the limits. Then from Eq. (13)

$$\lim_{\theta \to \pi} r(\theta) = \lim_{\theta \to \pi} \frac{-1}{gg' - 2f} = \frac{1}{4}.$$

The first equality uses the definition of F, after application of L'Hôpital's rule, and the second is an explicit evaluation of the resulting limit. A similar calculation shows that $\lim_{\theta \to -\pi} r(\theta) = 1/4$, so, in particular, $r(-\pi) = r(\pi)$ in the limit. Returning to the original scaling, the definition

$$\rho(-\pi) \equiv \frac{\sigma\rho_0}{2M} \equiv \rho(\pi) \tag{14}$$

along with Eq. (13) yields a continuous, 2π-periodic solution to the Fokker-Planck equation.

As an aside, since $\theta = \pi$ is the condition for the neuron to emit a spike, Eq. (14) also gives the steady-state mean spike rate of the neuron, although M and ρ_0 depend nontrivially on u and σ. Recently, Lindner *et al.* [20] used first passage time arguments to calculate the mean and coefficient of variation (the standard deviation divided by the mean) of the interspike interval distribution for this model. Future work combining these alternative expressions of the spike rate could simplify the analytic representation of the steady-state phase density.

B. LE calculation

To find the Lyapunov exponent (following [17], p. 474) of the stochastic forced theta neuron Eq. (2), consider its linearization

$$dv = f'(\theta(t))v\,dt + g'(\theta(t))v \circ dW \tag{15}$$

about a fixed solution $\theta(t)$. Then v satisfies

$$\begin{aligned} \ln|v(t)| &= \ln|v_0| + \int_0^t f'(\theta(s))ds + \int_0^t g'(\theta(s)) \circ dW_s \\ &= \ln|v_0| + \int_0^t \left(f'(\theta(s)) + \frac{1}{2} g(\theta(s)) g''(\theta(s)) \right) ds \\ &\quad + \int_0^t g'(\theta(s)) dW_s. \end{aligned} \tag{16}$$

The second equality is the conversion from the Stratonovich ($\circ dW$) to the Itô (dW) integral [22]. The average of the final Itô integral is zero as g' is bounded. Thus, using ergodicity of the system to equate the time average of the first integral with integration against the steady-state $\rho(\theta)$, the LE satisfies [17]

$$\lambda_w \equiv \lim_{t \to \infty} \frac{1}{t} \ln|v(t)| = \int_{-\pi}^{\pi} \left(f'(\eta) + \frac{1}{2} g(\eta) g''(\eta) \right) \rho(\eta) d\eta. \tag{17}$$

Numerical evaluation of this integral provides the LE (see the Appendix for additional numerical details).

IV. EFFECT OF FORCING AMPLITUDE

In the absence of forcing fluctuations, $\sigma = 0$, the *asynchronous* steady state is found directly from Eq. (5) as $\rho(\theta) = \sqrt{u}/[\pi f(\theta)]$ (scaled so that ρ has unit integral). By symmetry (or direct calculation), Eq. (17) thus shows that the LE is zero. Indeed, since the neuron is oscillatory, any perturbation to the asynchronous density oscillates at the natural period, indicating neutral stability.

A. LE for sinusoidal forcing

To provide a baseline for comparison when $\sigma > 0$, we numerically compute the LE for an ensemble entrained to sinusoidal forcing at the natural period (to our knowledge this has not been reported analytically, although it is closely related to the well-understood Hill equation [18]). Consider Eq. (1) with $I_{\text{app}} = u + \sigma\sqrt{2}\sin(2\pi t/T_N)$, where T_N is the natural period. The factor $\sqrt{2}$ normalizes the input variance to be σ^2. As above, the solution to the linearization of Eq. (1) about $\theta(t)$ is

$$\ln|v(t)| = \ln|v_0| + \int_0^t \tilde{f}(\theta(s), s) ds, \tag{18}$$

where $\tilde{f}(\theta, t) = [1 - I_{\text{app}}(t)]\sin(\theta)$. Suppose $\theta(t)$ is the stable 1:1 phase-locked solution. Then, using periodicity, the LE is

$$\lambda_p = \lim_{t \to \infty} \frac{1}{t} \ln|v(t)| = \frac{1}{T_N} \int_0^{T_N} \tilde{f}(\theta(s), s) ds. \tag{19}$$

Figure 1 (gray curve) shows λ_p computed across a range of σ. At first the LE decreases with increasing σ, indicating better entrainment. For higher σ the LE returns to zero, the 1:1 solution loses stability, and more complicated locking patterns occur. Note that I_{app} is strictly positive only for σ

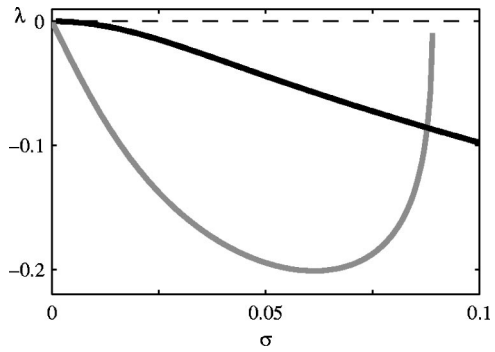

FIG. 1. The Lyapunov exponent for the theta model with sinusoidal (λ_p, gray) and white (λ_w, black) inputs, as a function of forcing amplitude. The mean input $u=0.01$.

$<u/\sqrt{2}\approx 0.007$. Above this value the forcing could be considered ''strong,'' as it transiently introduces fixed points in the model, Eq. (1).

B. LE for white forcing

For the white-forced theta neuron, the peak in the steady-state density ρ shifts to the left of the origin (Fig. 2) as σ increases, which we explain as follows. For increasing input fluctuation, the average frequency of the theta neuron increases (not shown), as the white input assists the neuron in escaping the slow region around the saddle node ghost at the origin [23]. This in turn increases the probability flow past the spike ($\theta=\pi$) and reinjects probability at negative θ. This process is asymmetric, because the escape of a neuron in the interval $[-\pi,0]$ can be significantly delayed by a more negative input, but a neuron that has begun to spike will continue through $\theta=\pi$ independent of the input. Heuristically, most of the ensemble is ''waiting'' to get past the origin, and neurons that make it past the saddle node ghost almost immediately return to waiting, thereby shifting the density peak into the ''repolarization'' interval $[-\pi,0]$. While a similar behavior has been inferred in phase models before [12], the author is not aware of a previous attempt to explain its cause.

For θ in $[-\pi,0]$, the divergence of the SDE is negative (that is, $d/d\theta(d\theta/dt)<0$). The shift of the ensemble density thus induces a contraction of nearby solutions. To quantify the contraction, Eq. (17) is used to numerically compute the LE λ_w for a range of forcing strengths σ, shown in Fig. 1 (black curve). As expected, the exponent is negative, suggesting solutions asymptotically approach each other, and is monotonically decreasing, so that stronger forcing results in faster (more stable) synchronization. However, as σ goes to zero, the curve of λ_w approaches tangentially to the σ axis, so that synchronization is weak for a nontrivial range of forcing amplitude.

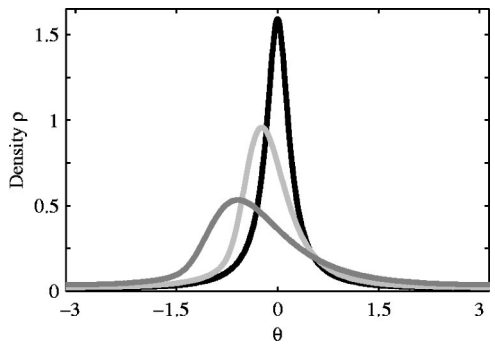

FIG. 2. Steady-state densities ρ for $\sigma=0$ (black), 0.1 (light gray), and 0.3 (dark gray). The mean input $u=0.01$.

C. Comparison of forcing types

The fair comparison of a sinusoid input with a white signal is a subtle question. A usual control is to match the fluctuation power (time average of the squared input fluctuations) between different input types [7–9]. For a stationary process the power equals the variance around any fixed time point. However, $\circ dW$ is a generalized process, and the variance at each time point is infinite [22]. Indeed, the term ''white'' denotes that the signal contains equal (positive) energy at all frequencies; since the power is equal to the integral of the spectrum, the power is also infinite [22]. Thus, although the white signal has an intensity σ, it is not obvious how this number should be scaled to compare to an input with finite power.

Recall that white forcing arose as an idealization of a broadband input current due to the summation of many independent inputs. In practice this input will be band limited and of finite power. The approximation used here is valid when the highest frequency in the input signal is well above the fastest time scale of the system, and implicit in this approach is a scaling that depends in a complicated way on the system being stimulated [9,22,24]. Through such a scaling, we could compare the magnitude of $\lambda_p(\sigma)$ directly with a modified white forced LE, $\tilde{\lambda}_w(\sigma)\equiv\lambda_w(\alpha\sigma)$, where α is system dependent.

However, an important qualitative aspect of Fig. 1 persists under any reasonable scale. In particular, because the slope of λ_w approaches zero as $\sigma\to 0$, at small forcings we must have $\tilde{\lambda}_w>\lambda_p$. Further, because $\tilde{\lambda}_w$ is monotonically decreasing but λ_p is not, we also have that, at sufficiently high σ, $\tilde{\lambda}_w<\lambda_p$. Thus there is an amplitude dependent transition between greater reliability to periodic input (at the natural frequency) for low σ, and greater reliability to broadband input at high σ, as measured by the LE. This behavior is especially interesting in comparison with the experimental demonstration of resonance reliability (that is, frequency dependence of reliability) only for a range of forcing amplitudes [7,9].

We note that for high-amplitude white forcing, coherent oscillations are lost and the neuron approaches a refractory Poisson process (unpublished; see also [20,25]). For example, at the highest σ in Fig. 1, $\sigma=0.1$, the coefficient of variation of the interspike interval distribution is approximately 0.5, indicating fairly irregular spike timing. The plotted range of σ extends into ''strong'' white forcing [20] (and strong sinusoidal forcing, given the loss of stability of 1:1 entrainment), and the two LE curves should be qualitatively comparable.

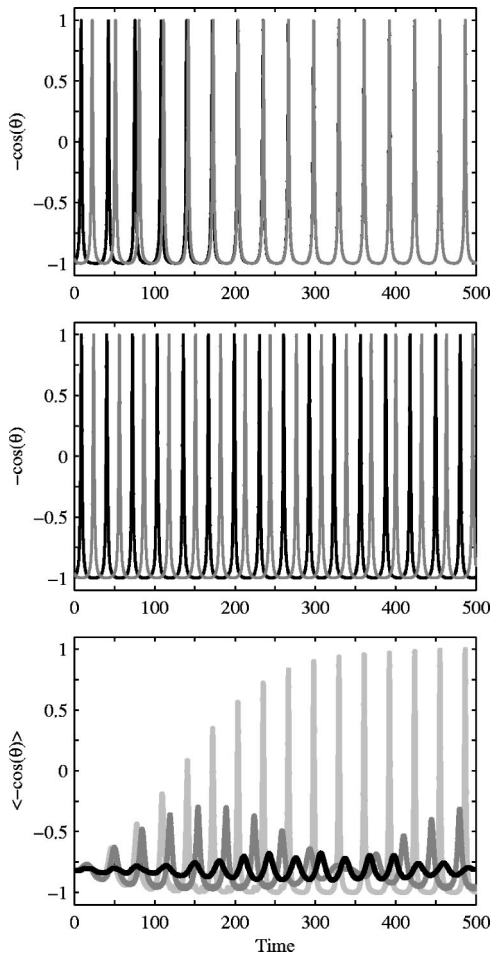

FIG. 3. Top. Two example solutions, with near-antiphase initial conditions, of the theta neuron weakly forced by a sinusoid at the natural frequency. Middle. The same but with a single realization of white forcing. Bottom. Ensemble average of 50 solutions starting from an asynchronous (splay) state, for three different inputs: white forcing (black), sinusoid at the natural period T_N (light gray), and sinusoid with period $T_N/0.87$ (dark gray). Solutions were computed via the Euler method for Eq. (1) or Eq. (4) with $u=0.01$, $\sigma=0.0025$, and time step $\Delta t=10^{-4}$.

D. Time evolution of synchronization

As a further example of the greater efficacy of sinusoidal forcing at low amplitudes, Fig. 3 demonstrates the neural response to three different forcing regimes, with $\sigma=0.0025$. To make the spike times more apparent, we plot $-\cos[\theta(t)]$ for each neuron [25]; this function is near -1 around rest ($\theta=0$), and is $+1$ at the spike ($\theta=\pi$). Figure 3, top, shows two neurons with near-antiphase initial conditions receiving a common sinusoid input at the natural frequency (as in Sec. IV A). They quickly approach a common solution. The light gray curve in Fig. 3, bottom, shows the ensemble average over 50 neurons with asynchronous initial conditions. For an asynchronous ensemble the average is a constant, $\langle -\cos(\theta)\rangle \sim -0.82$ (the mean value of $-\cos[\theta(t)]$ for a single unforced oscillator). However, under the forcing the ensemble average quickly approaches the wave form of a single solution, showing synchronization of the entire ensemble.

The dark gray curve of Fig. 3, bottom, shows the ensemble average when the forcing is replaced by a sinusoid with period $T_N/0.87$, chosen to lie just outside the 1:1 Arnold tongue. Individual solutions are quasiperiodic, and the ensemble average shows beating. Thus, although there are short time epochs in which the ensemble is nearly clustered (e.g., around $t=150$), further input disrupts these clusters and there is no asymptotic approach to a common solution.

White forcing shows a combination of these behaviors. At this forcing amplitude, changes in relative phase are not apparent in individual neurons (Fig. 3, middle). Some tendency toward clustering is visible in the ensemble (Fig. 3, bottom, black curve), and since the LE is negative, the ensemble will eventually approach a common solution as $t\to\infty$. However, it does so in a biased random walk fashion, with epochs of increased clustering (e.g., around $t=300$) interspersed with epochs of desynchronization (e.g., around $t=450$). A detailed examination of the synchronization dynamics shows that the negativity of the LE is due to rare but highly synchronizing epochs outweighing a smaller unbiased walk in the level of synchronization [13]. This behavior is similar to that observed in phase oscillators driven by a sinusoidal input with slow, random frequency modulation [11]. The important observation is that the nervous system often operates on time scales of a few spikes, so that, independent of the LE, the fluctuation in the degree of synchronization could also be functionally relevant. In contrast to the monotone approach to synchrony under sinusoidal input, white forcing can in fact desynchronize the ensemble on short time scales.

V. CONCLUSION

Motivated by the phenomenon of neural response reliability, we have modeled a simple neural oscillator forced by a broadband input. We have not explicitly modeled the reduction in reliability from intrinsic noise, e.g., due to ion channel fluctuations [10,16]. We instead focused on the dynamical stability of the nonautonomous neuron with input, and expect synchronization to persist under small intrinsic noise. However, because the effect of noise can be state dependent [10], the extension of our analysis to models with intrinsic noise could reveal interesting behaviors.

As in the case of scalar equations on the real line ([17], p. 473) and additive noise on the circle ([17], p. 398), [12], white forcing here induces a negative LE, and thus almost all solutions should converge asymptotically. In [12], a Poincaré map is used to show directly that the negative LE leads to synchronization in an active rotator with additive white forcing. An almost identical argument holds for the theta neuron in this paper. However, [12] relied on general results in [17] without actually determining the steady-state phase distribution, the magnitude of the LE, or the time course of synchronization for reasonable forcing amplitudes. By calculating the steady-state distribution to get a semianalytic expression for the LE, it is shown here that the LE remains small, relative to periodic input, for a range of amplitudes. Thus, although the system may ultimately synchronize under white forcing, it may take a physiologically untenable amount of time to do so, and other inputs may be more effective. In

particular, for low forcing strengths the spectrum of the input may dominate entrainment behavior [7,9].

Periodic inputs at frequencies not harmonically related to the natural period result in transient and partial clustering of an initially asynchronous ensemble (as in Fig. 3, bottom, dark gray); this is the ensemble level manifestation of the classical result that individual solutions are quasiperiodic and neutrally stable. In this case, even small intrinsic noise would accumulate and lead to unreliable spike times [16]. Even when solutions are entrained, an argument for the importance of aperiodicity in inducing reliable responses is that higher-order locking in periodically forced systems can obstruct ensemble synchronization [14,16]. For example, under stable 2:1 phase locking, an initially asynchronous ensemble splits into two clusters, separated in time by one input period. Although information about the input is preserved at the population level, the spike times for a single neuron depend on initial conditions (and on noise mediated jumps between clusters) and hence are unreliable [16]. However, especially for low forcing strengths, the most common form of phase locking is 1:1, in which multiple clusters do not exist. In higher-dimensional models, moreover, even aperiodic inputs can lead to multiple clustering (unpublished; and, e.g., the bistable regime of [15]), a behavior that is observed experimentally [3,4]. A full understanding of reliability requires conditions not only on the input, but also on the dynamical details of the neural model. This includes an examination of the temporal fluctuation in reliability, as is observed for both anharmonic sinusoidal forcing and white forcing (Fig. 3, bottom; see also [13]).

In other work with the theta neuron model, we found that broadband inputs filtered at the natural frequency do not produce reliable spiking [13], in more direct correspondence to the results of [7,9]. As shown in this paper by the comparison of broadband with periodic inputs, temporal structure in the input can be a major determinant of reliability for systems with a defined time scale (e.g., the oscillation period).

ACKNOWLEDGMENTS

The author thanks Nancy Kopell, Bard Ermentrout, John Rinzel, Mark Andermann, and Margaret Beck for spirited discussions and helpful comments. The author was supported by the Burroughs-Wellcome Fund Program in Mathematical and Computational Neuroscience at Boston University.

APPENDIX: NUMERICAL EVALUATION OF THE STEADY STATE

The numerical usefulness of Eq. (13) is tempered by the fact that it contains quotients of large valued functions. Thus, although the final value of ρ may be small, the intermediate steps are numerically out of machine range [the problem persists under the change of coordinates $z=\tan(\theta/2)$]. It is easier to numerically solve the first order differential equation Eq. (7), but C must be chosen correctly for this first order solution to match the boundary conditions of the original second order problem Eq. (6). The crucial observation is that C was determined [Eq. (12)] during the derivation of the analytic solution, and moreover can be calculated directly from the theta neuron vector field (to get M) and the arbitrary choice of scaling $\rho_0=1$. After a solution is computed it can be normalized to have unit integral.

$M=\int_0^\pi \mu$ is numerically evaluated first, to high precision (note that μ goes rapidly to zero for positive θ). We then rearrange Eq. (7) as

$$\frac{d\rho}{d\theta}=\frac{2}{g^2}\left[\left(f-\frac{1}{2}g\frac{dg}{d\theta}\right)\rho-\frac{\sigma\rho_0}{M}\right]\equiv G(\theta)\left(A(\theta)\rho-\frac{\sigma\rho_0}{M}\right) \tag{A1}$$

on $I=(-\pi,\pi)$. Since $G(\theta)A(\theta)>0$ for u, σ, and θ of interest, integration of Eq. (A1) is stable when integrated backward (decreasing θ). The prefactor G goes rapidly to infinity at both edges of the interval, making even the backward (stable) integration ill posed for most numerical solvers. However, when G is large, ρ is approximately equal to the algebraic value obtained by setting the parenthetical term on the right hand side of Eq. (A1) to zero ($d\rho/d\theta$ is of order 1).

We thus split I into ''inner'' and ''outer'' intervals, by choosing a positive value θ^* for which $G(\theta^*)\gg 1$ [specifically $G(\theta^*)=10G(0)=5/\sigma^2$]. The inner region I_{in} is defined by $|\theta|<\theta^*$, and the outer region I_{out} is the complement. On I_{out}, Eq. (A1) yields the approximation

$$\rho(\theta)=\frac{\sigma\rho_0}{M[f(\theta)-g(\theta)g'(\theta)/2]}. \tag{A2}$$

Note that this expression agrees with the earlier determined values Eq. (14) at the end points. We numerically integrated the ordinary differential equation Eq. (A1) backward from θ^* to $-\theta^*$, using the starting value given by the outer approximation. As a self-consistency check, the integrated solution (before normalization) should agree both with $\rho_0=1$ at the origin and with the outer solution at $-\theta^*$. For the figures presented here, mismatch errors at these two points were of order 10^{-5}. Moreover, direct simulation, for a subset of parameter values, of the SDE Eq. (4) using Euler's method produced good agreement with the analytical curves, but with substantially longer computation time (not shown; numerical solution appeared convergent near $dt=10^{-4}$).

[1] W.R. Softky and C. Koch, J. Neurosci. **13**, 334 (1993).
[2] A. Destexhe, M. Rudolph, J.M. Fellous, and T.J. Sejnowski, Neuroscience **107**, 13 (2001).
[3] Z.F. Mainen and T.J. Sejnowski, Science **268**, 1503 (1995).
[4] H.L. Bryant and J.P. Segundo, J. Physiol. (London) **260**, 279 (1976).
[5] L.G. Nowak, M.V. Sanchez-Vives, and D.A. McCormick, Cereb. Cortex **7**, 487 (1997).
[6] R.R. de Ruyter van Steveninck, G.D. Lewen, S.P. Strong, R. Koberle, and W. Bialek, Science **275**, 1805 (1997).

[7] J.D. Hunter, J.G. Milton, P.J. Thomas, and J.D. Cowan, J. Neurophysiol. **80**, 1427 (1998).
[8] J.S. Haas and J.A. White, J. Neurophysiol. **88**, 2422 (2002).
[9] J.D. Hunter and J.G. Milton, J. Neurophysiol. **90**, 387 (2003).
[10] E. Schneidman, B. Freedman, and I. Segev, Neural Comput. **10**, 1679 (1998).
[11] R.V. Jensen, Phys. Rev. E **58**, R6907 (1998).
[12] K. Pakdaman, Neural Comput. **14**, 781 (2002).
[13] J. Ritt, Ph.D. thesis, Boston University, 2003.
[14] P.H. Tiesinga, Phys. Rev. E **65**, 041913 (2002).
[15] E.K. Kosmidis and K. Pakdaman, J. Comput. Neurosci. **14**, 5 (2003).
[16] R. Brette and E. Guigon, Neural Comput. **15**, 279 (2003).
[17] L. Arnold, *Random Dynamical Systems* (Springer-Verlag, Berlin, 1998).
[18] G.B. Ermentrout and N. Kopell, SIAM J. Math. Anal. **46**, 233 (1986).
[19] B. Ermentrout, Neural Comput. **8**, 979 (1996).
[20] B. Lindner, A. Longtin, and A. Bulsara, Neural Comput. **15**, 1761 (2003).
[21] S.H. Strogatz, *Nonlinear Dynamics and Chaos* (Addison-Wesley, Reading, MA, 1994).
[22] C.W. Gardiner, *Handbook of Stochastic Methods* (Springer-Verlag, Berlin, 1985).
[23] W.-J. Rappel and S.H. Strogatz, Phys. Rev. E **50**, 3249 (1994).
[24] M. Litong, Y. Hayakawa, and Y. Sawada, Phys. Rev. E **64**, 026117 (2001).
[25] B.S. Gutkin and G.B. Ermentrout, Neural Comput. **10**, 1047 (1998).